FACTA UNIVERSITATIS (NIŠ)
Series: Electronics and Energetics vol. 12, No.2 (1999), 187-207

UDC 621.391:681.32

SELECTIVE LINEAR PHASE DIGITAL FILTERS: THEORY AND APPLICATION

This paper is dedicated to Prof. Ilija Stojanović on the occasion of his 75^{th} birthday and the 50^{th} anniversary of his scientific work

Ljiljana D. Milić and Miroslav D. Lutovac

Abstract. This paper reviews the exact and approximate linear phase IIR filter designs based on the classical approximating functions (elliptic, Butterworth and Chebyshev type functions) and the usage of various processing techniques. Using allpass IIR subfilters obtained from the minimal phase solution, it is possible to implement a causal filter which exhibits simultaneously an approximate constant amplitude response and an exact or approximate linear phase response.

1. Introduction

A digital filter having a linear phase response, sharp magnitude response and a small number of multiplications per output sample is a very desirable cost-effective realization.

A precise linear phase transfer function can be easily realized as an FIR filter. Unfortunately, the linear phase FIR filter requires many times more multiplications per output sample than an IIR filter to satisfy a sharp magnitude response specification. On the other hand, the IIR filter cannot be designed to exhibit an exact linear phase. Even more, IIR filters have very nonlinear phase responses. Fortunately, an approximate linear phase IIR filter can be realized using the classical filter transfer functions and the time-reversed techniques.

Alternatively, a nonlinear phase IIR filter, $H(z)$, can be followed by allpass phase equalization so that the overall transfer function has the same

Manuscript received September 14, 1999.

Lj. D. Milić is with Mihajlo Pupin Institute, Volgina 15, 11050 Belgrade, Yugoslavia, e-mail: emilicl@ubbg.etf.bg.ac.yu and M. D. Lutovac is with IRITEL, Batajnički put 23, 11080 Belgrade, Yugoslavia, e-mail: lutovac@iritel.bg.ac.yu .

magnitude response as $H(z)$, and an approximate linear phase or a flat group delay in the frequency range of interest [1]. Usually, this realization results in more multiplies per sample than an FIR filter [2] and it is not analyzed in this paper. Also, optimization can be used to simultaneously approximate both magnitude and phase response specifications [3], [4], [5], [6], [7], [8], with fewer multiplications than corresponding FIR filters. This approach usually gives an economical solution, but requires the exhaustive iterative procedure and sometimes has the problems with convergence.

This paper presents a new approach for designing approximate linear phase IIR filters. The proposed approach is based on the classical approximating functions (elliptic, Butterworth and Chebyshev type functions). The computation procedure does not require any optimization and therefore is very fast.

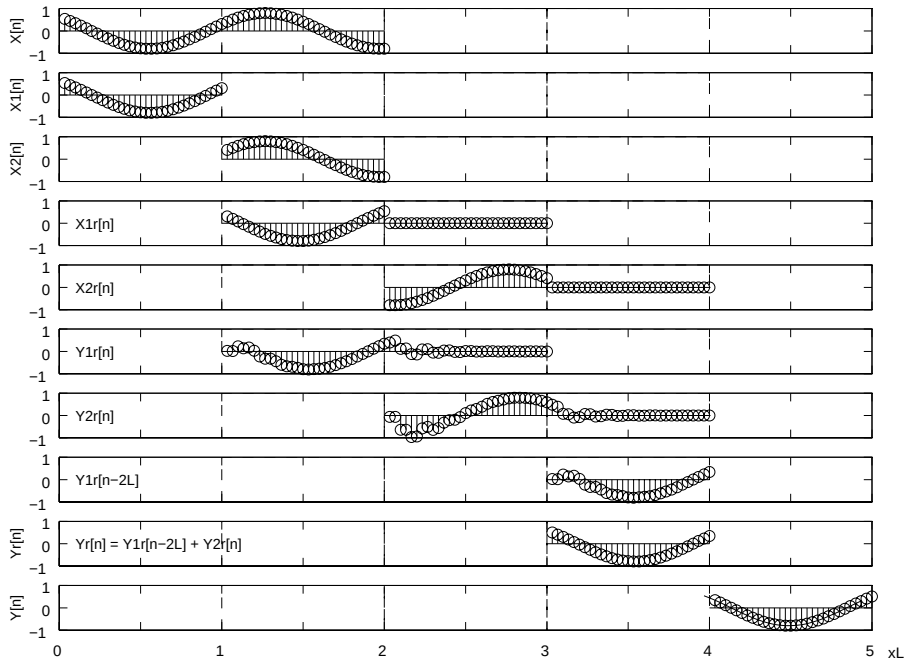

Fig. 1. Block processing sequences with L sample long block sequences.

In general, the linear phase IIR filter has to realize a transfer function or a partial transfer function $H_a(z)H_b(z^{-1})$, where $H_a(z)$ and $H_b(z)$ have the poles with radii smaller than one. This means that $H_b(z^{-1})$ has poles with

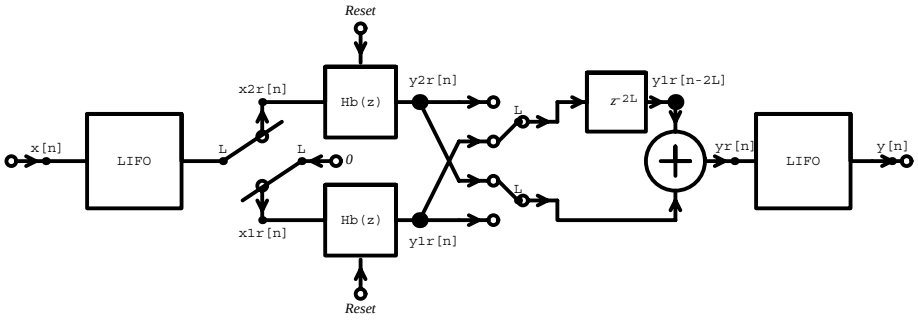

Fig. 2. Block diagram implementations of noncausal transfer function $H_b(z^{-1})$ using the causal filter $H_b(z)$ and block processing technique.

radii greater than one, and thus H_b subfilter is unstable. Several techniques have been suggested to realize $H_b(z^{-1})$ using causal filters:

- The *time reversed technique* can be used for realizations where filtering is permissible off-line [9], [10]: (1) time reverse an input sequence $x[n]$ and create a reversed sequence $x[-n]$, (2) create the output sequence $y[-n]$ by employing causal filter $H_b(z)$ whose input is the sequence $x[-n]$, (3) time reverse output sequence $y[-n]$ and create $y[n]$. Finally, the output sequence $y[n]$ is filtered sequence $x[n]$ by noncausal filters $H_b(z^{-1})$, but it is created using causal filter $H_b(z)$. The advantages of using the time reversed IIR filter technique versus FIR filters were presented in [10], [11], [12], [13], [14], [3].
- The *block processing technique* can be used for real-time implementations and the processing of the infinite length or very long finite input sequences [15]. The infinite length input sequence is divided into L-length sequences and each sequence is filtered separately: (1) the input L-length sequence, $x_2[n]$, is stored into *last-in first-out* (LIFO) register; (2) the time-reversed sequence, $x_{2r}[n]$, is filtered using filter H_b yielding $2L-$length output sequence $y_{2r}[n]$; (3) the sum of the last L output samples of y_{2r} and the first L output samples of the previous sequence, $y_{r1}[n]$, (delayed $2L$ samples) is a new sequence $y_r[n]$; (4) the $L-$length sequence $y_r[n]$ is time reversed using LIFO register creating $y[n]$, Figs. 1 and 2. The noncausal filtering using H_b can be performed before [15] or after [11], [12], [13], [14] filter H_a. This technique may require a large data storage and processing delay. The phase tolerance is smaller for larger L.

- A FIR filter is created using the impulse response of IIR filter whose transfer function is $H_a(z)H_b(z^{-1})$. The length of this FIR filter can be larger than the length of the optimal linear phase FIR filter. Moreover, the phase response is only approximately linear. The phase tolerance can be decreased by increasing the length of the FIR filter.
- A FIR filter is created using the impulse response of noncausal IIR filter whose transfer function is $H_b(z^{-1})$. The length of this FIR filter can be much smaller than the length of the optimal linear phase FIR filter while the storage requirement is smaller than the storage of block processing technique. The number of multipliers of FIR filter is increased, but it is still smaller than it appears in optimal linear phase FIR filters.
- The computational cost of the FIR realization can be reduced by creating a new IIR filter starting from the impulse response and using Prony method. This method increases the error of phase responses.

2. Exact Linear Phase Transfer Function

In theory, the exact linear phase transfer function $H(z)$ can be obtained as a product of two transfer functions

$$H(z) = H_c(z)H_d(z^{-1}), \tag{1}$$

where

1. the transfer functions are identical $H_c(z) = H_d(z)$, or
2. the transfer functions have the identical poles while all zeros lie on the unit circle.

The exact linear phase IIR filter can be designed using standard magnitude-only IIR filter design programs and the magnitude response is equal to $|H_c(e^{j2\pi f})|^2$ for $H_c(z) = H_d(z)$. If $H_c(z)$ and $H_d(z)$ are elliptic IIR transfer functions, $H_c(z) = H_d(z)$, than the same linear-phase design specification with an additional 6dB stopband attenuation will be met if the poles of $H_c(z) = A(z)/D(z)$ and $H_d(z) = B(z)/D(z)$ are not identical [16] although the design program is also based on the classical Jacobi elliptic functions.

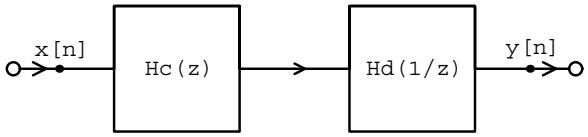

Fig. 3. Block diagram implementations of exact linear phase transfer function using elliptic filters $H_c(z)$ and $H_d(z)$.

The block diagram implementation of an exact linear phase transfer function is shown in Fig. 3. The implementation yields only an approximate linear phase response because the errors are inevitable in the implementation due to the finite wordlength and the finite block sequence length L while the impulse response of IIR filter $H_d(z)$ has an infinite length. A larger L yields a smaller phase error but also a larger processing delay. The minimal phase error is for L equal to the input sequence length, but in that case, the processing delay is maximal.

3. Approximate Linear Phase Transfer Function

An approximate linear phase transfer function $H(z)$ can be obtained from a minimum phase odd-order elliptic IIR filter $H_e(z)$

$$H_e(z) = \frac{1}{2}\left(H_a(z) + H_b(z)\right) \tag{2}$$

where $H_a(z)$ and $H_b(z)$ are allpass transfer functions [17]

$$\begin{aligned} H_a\left(e^{j\omega}\right) &= e^{j\varphi_a(\omega)} \\ H_b\left(e^{j\omega}\right) &= e^{j\varphi_b(\omega)} \end{aligned} \tag{3}$$

The allpass IIR filters $H_a(z)$ and $H_b(z)$ are the causal allpass subfilters, and they can be designed using standard magnitude-only IIR filter design programs [17] because the poles of $H_a(z)$ and $H_b(z)$ are also the poles of the odd-order elliptic IIR filter $H_e(z)$. This way, minimum phase IIR filter $H_e(z)$ is obtained. The implementation of $H_e(z)$ based on equation (2) is shown in Fig. 4.

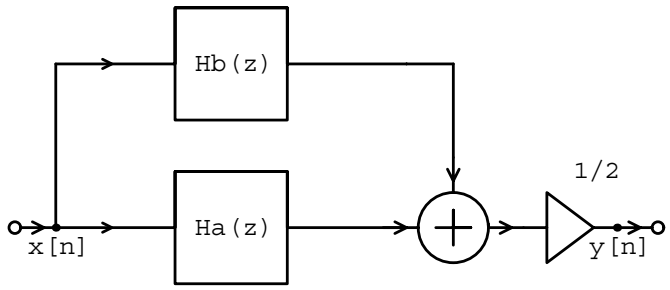

Fig. 4. Block diagram implementations of elliptic transfer function $H_e(z) = \frac{1}{2}\left(H_a(z) + H_b(z)\right)$ using allpass filters $H_a(z)$ and $H_b(z)$.

The approximate linear phase transfer function $H(z)$

$$H(z) = \frac{1}{2}\left(1 + H_a(z)H_b(z^{-1})\right) \tag{4}$$

can be derived from the minimum phase transfer function $H_e(z)$

$$H(z) = H_b(z^{-1})H_e(z) = \frac{1}{2}\left(1 + H_a(z)H_b(z^{-1})\right) \tag{5}$$

because for the allpass transfer function $H_b(z)$, it can be shown that $H_b(z)H_b(z^{-1}) = 1$, i.e. $H_b(e^{j\omega})H_b(e^{-j\omega}) = e^{j\varphi_b(\omega)}e^{-j\varphi_b(\omega)} = e^0 = 1$.

The causal implementation of the noncausal transfer function $H_b(z^{-1})$, such as the realization based on the time reversed technique or the block processing technique, requires a processing delay, say m samples. Therefore, the causal implementation of the transfer function $H(z)$ requires also the processing delay of m samples

$$z^{-m}H(z) = \frac{1}{2}\left(z^{-m} + H_a(z)\ \ \left(z^{-m}H_b(z^{-1})\right)\right) \tag{6}$$

where $z^{-m}H_b(z^{-1})$ is implemented using the causal filter $H_b(z)$ while the delay z^{-m} is the delay produced by the LIFO registers.

The causal implementation of an approximate linear phase transfer function is shown in Fig. 5, where $H_b(z^{-1})$ is implemented employing causal filter $H_b(z)$ as shown in Figs. 6 and 2.

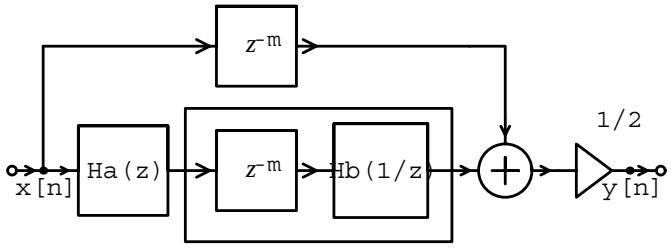

Fig. 5. Block diagram implementations of approximate linear phase transfer function using allpass filters $H_a(z)$ and $H_b(z)$.

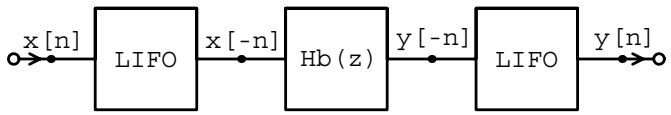

Fig. 6. Block diagram implementations of noncausal transfer function $H_b(z^{-1})$ using the causal filter $H_b(z)$ and time reversed technique.

The filter frequency response can be expressed as a product of the amplitude function, $\cos(\Psi(\omega))$, and the exponential factor, $e^{j\Psi(\omega)}$,

$$\begin{aligned} H\left(e^{j\omega}\right) &= \cos\left(\Psi\left(\omega\right)\right) e^{j\Psi(\omega)} \\ \Psi\left(\omega\right) &= \frac{\varphi_a\left(\omega\right) - \varphi_b\left(\omega\right)}{2} \end{aligned} \tag{7}$$

where $\Psi(\omega)$ is the phase response. The passband is obtained for $\left|H\left(e^{j\omega}\right)\right| \approx 1$, i.e. for $\cos(\Psi(\omega)) \approx 1$ or $\Psi(\omega) \approx 0$, while $\left|H\left(e^{j\omega}\right)\right| \approx 0$, or $\cos(\Psi(\omega)) \approx 0$, or $\Psi(\omega) \approx \pi/2$ gives the stopband. Evidently, an equalripple behavior of the amplitude response produces simultaneously an equalripple behavior of the phase response and vice versa, as it is shown in Fig. 7.

The passband phase tolerance $\Delta\psi$ can be expressed in terms of the maximal passband attenuation A_p (dB)

$$\Delta\psi = \cos^{-1}(10^{-A_p/20}) \tag{8}$$

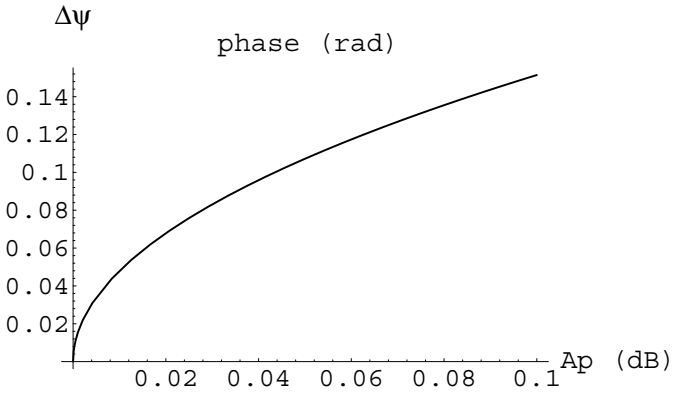

Fig. 7. Passband phase tolerance $\Delta\psi$ in rad vs. maximal passband attenuation A_p in dB for approximate linear phase filters.

A very small passband attenuation yields a very small deviation of the phase response from the linear function. This implies that an EMQF filter (Elliptic Minimal Q Factor) [17], that has a very small passband ripple, is an excellent choice for designing the approximate linear phase filter.

4. Time Reversed Technique

From sections 2 and 3, it is evident that for the exact linear phase or for the approximate linear phase design, the noncausal filtering has to be

performed. The time reversed technique can be used for the realization of the noncausal filter $H_b(z^{-1})$ using causal filter $H_b(z)$, Fig. 6. The advantages of using time reversed IIR filter technique versus FIR filters were presented in [10], [11], [12], [13], [14], [3]. The connection of filters $H_a(z)$ and filter $H_b(z)$ realized using the time reversed technique is also called a zero-phase filter and it has an exact phase linearity. The MATLAB implements this zero-phase filter using `filtfilt.m` file. After filtering in the forward direction using $H_a(z)$, the filtered sequence is then reversed and run back through the same filter $H_b(z)$=$H_a(z)$. The resulting sequence has a precisely zero-phase response, and the filter order is doubled, $|H_a(z)|^2$. Care is taken to minimize startup and ending transients by matching initial conditions. The length of the input sequence must be more than three times the order of the filter $H_a(z)$.

5. Block Processing Technique

The block processing technique can be used for real-time implementations of the noncausal filter $H_b(z^{-1})$ using causal filter $H_b(z)$. It can be used for the processing of the infinite length sequences or very long finite input sequences [15]. The input sequence is divided into $L-$length sequences and each sequence is filtered separately as shown in Figs. 1 and 2. The noncausal filtering using H_b can be performed before [15] or after [11], [12], [13], [14] filter H_a. The storage and processing delay is smaller for a smaller L.

Powell and Chau have devised two methods [15]: (1) overlap-save and (2) overlap-add method. The causal transfer function $H_a(z)$ can be also implemented using the block processing technique, but without LIFO registers, and this way Powell and Chau realize a limit cycle free implementation [15].

When a sine input sequence is used, the total harmonic distortion due to the finite sequence length L depends also on the numerator associated with $H_a(z)$ or $H_b(z)$ [18].

6. FIR Implementation of Allpass Subfilter

It is shown in section 3 that we can replace the block processing technique by an appropriate FIR subfilter. The FIR subfilter is created using the main part of the impulse response of the IIR allpass filter whose transfer function is $H_a(z)H_b(z^{-1})$ where $H_a(z)$ and $H_b(z)$ are allpass functions from the minimum phase solution. By employing the finite length FIR filter we approximate the infinite length impulse response of the IIR filter. The length of this FIR filter can be larger than the length of the optimal linear

phase FIR filter. Moreover, the phase response is only approximately linear. The phase tolerance is smaller for the higher-order FIR filters.

The best cost-effective filter implementation employs the allpass first-order and the second-order subfilters, because it requires the minimal number of multipliers per subfilter. Furthermore, the exact and approximate linear phase transfer function can be implemented using the allpass subfilters as shown in Figs. 4 and 5. Hence, we analyze the impulse response of the first-order, $H_1(z)$, and the second order, $H_2(z)$, allpass IIR subfilter

$$\begin{aligned} H_1(z) =& \frac{p - z^{-1}}{1 - pz^{-1}} \\ H_2(z) =& \frac{\rho^2 - 2\rho\cos\theta + z^{-2}}{1 - 2\rho\cos\theta + \rho^2 z^{-2}} \end{aligned} \tag{9}$$

The impulse response of the first-order allpass IIR subfilter, $h_1(n)$, can be expressed in the following form

$$h_1[n] = p^n \left(p - p^{-1}\right) u[n] + p^{-1}\delta[n] \tag{10}$$

where $u[n]$ is the unit step sequence and $\delta[n]$ is the unit impulse sequence. The impulse response of the first-order allpass IIR subfilter is a decreasing function in n as shown in Fig. 8 for three different poles p, $|p| < 1$. The impulse response decreases faster for poles $p \approx 0$ due to the factor p^n, while the impulse response is very small for poles $p \approx \pm 1$ due to the factor $\left(p - p^{-1}\right)$.

For a given pole p, the magnitude of the impulse response is smaller than a prescribed acceptable error ϵ_n

$$|h_1[n_e]| \leq \epsilon_n, \; n_e > 1 \tag{11}$$

We find that the nth-sample satisfying condition (11) can be calculated as n_e

$$n_e \geq \frac{\log\left(\dfrac{\epsilon_n}{p^{-1} - p}\right)}{\log(p)} \tag{12}$$

Alternatively, for a given n_e, we can derive the pole value that yields the maximal amplitude of the impulse response

$$|h_1[n_e]|_{\max} = 2\sqrt{\frac{(n_e - 1)^{n_e - 1}}{(n_e + 1)^{n_e + 1}}}, \tag{13}$$

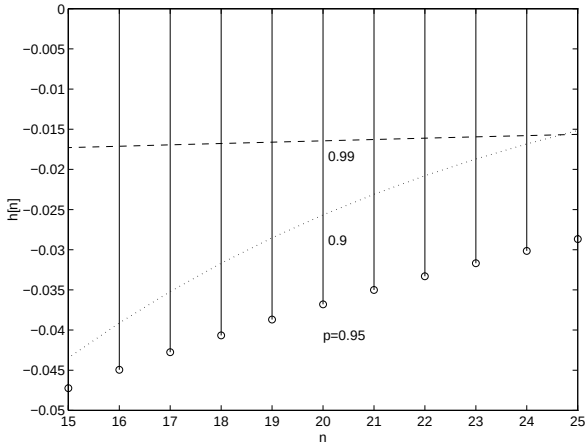

Fig. 8. Impulse response of the first-order allpass transfer function $H_1(z) = (p - z^{-1})(1 - pz^{-1})$*: the amplitude of the impulse response at* $n = 20$ *for* $p = 0.95$ *is larger than the amplitude of the impulse response for* $p = 0.9$ *(dotted line) and* $p = 0.99$ *(dashed line).*

for

$$p = \sqrt{\frac{n_e - 1}{n_e + 1}}$$

The impulse response of the second-order allpass IIR subfilter, $h_2(n)$, can be expressed in the following form

$$\begin{aligned} h_2[n] =& \rho^{-2}\delta[n] + \\ &+ \rho^n \left(1 - \rho^{-2}\right) \left(\rho^2 \frac{\sigma((n+1)\,\theta)}{\sin(\theta)} - \frac{\sin((n-1)\,\theta)}{\sin(\theta)}\right) u[n] \end{aligned} \tag{14}$$

The impulse response of the second-order allpass IIR subfilter is a sinusoidal function with a decreasing amplitude, as shown in Fig. 9, for three different pole magnitudes ρ, $|\rho| < 1$. The impulse response decreases faster for poles with $\rho \approx 0$ due to the factor ρ^n, while the impulse response is very small for poles with $\rho \approx \pm 1$ due to the factor $\left(\rho - \rho^{-1}\right)$.

For a given pole pair $p_1 = \rho e^{j\theta}$, $p_2 = \rho e^{-j\theta}$, the magnitude of the impulse response is smaller than a prescribed acceptable error ϵ_n

$$|h_2[n_e]| \leq \epsilon_n,\ n_e > 1 \tag{15}$$

We find that the nth-sample satisfying condition (15) can be approximately

calculated as n_e

$$n_e > \frac{\log\left(\dfrac{\epsilon_n}{2\left(\rho^{-1}-\rho\right)}\right)}{\log\left(\rho\right)} \tag{16}$$

Alternatively, for a given n_e, we can derive the pole value that yields the maximal amplitude of the impulse response

$$|h_2[n_e]|_{\max} \approx 4\sqrt{\frac{(n_e-1)^{n_e-1}}{(n_e+1)^{n_e+1}}}, \tag{17}$$

for

$$\rho \approx \sqrt{\frac{n_e-1}{n_e+1}}$$

It should be noticed that the derived relations are only approximate since the impulse response is a sinusoidal function and we assume that the argument θ is such that at n_e a sinusoidal function has its maximum.

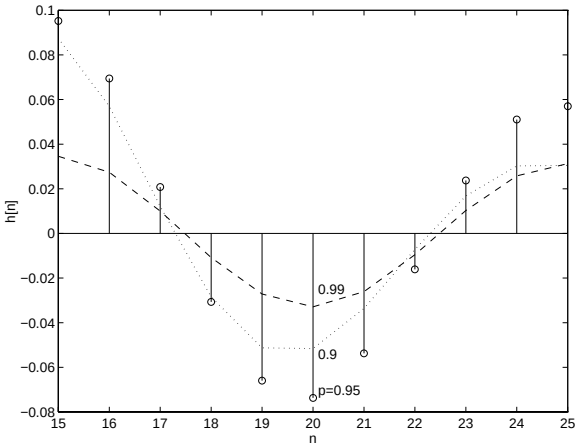

Fig. 9. Impulse response of the second-order allpass transfer function $H_2(z) = (\rho^2 - 2\rho\cos\theta + z^{-2})(1 - 2\rho\cos\theta + \rho^2 z^{-2})$, $\theta = -\pi/5$: *the amplitude of the impulse response at* $n = 20$ *for* $\rho \approx 0.95$ *is larger than the amplitude of the impulse response for* $\rho = 0.9$ *(dotted line) and* $\rho = 0.99$ *(dashed line).*

The impulse response amplitude of the second-order filter is approximately two times larger than the impulse response amplitude of the first-order filter for $\rho = p$.

7. FIR Implementation of Noncausal Subfilter

A FIR filter can be used to implement the noncausal allpass function $H_b(z^{-1})$, rather than the whole allpass function $H_a(z)H_b(z^{-1})$. The length of this FIR filter can be much smaller than the length of the optimal linear phase FIR filter while the storage requirement is smaller than the storage of block processing technique. The number of multipliers of FIR filter is increased, but it is still smaller than it appears in optimal linear phase FIR filters.

The allpass functions $H_a(z)$ and $H_b(z)$ can be calculated using a simple procedure:

- use a standard IIR filter design program for elliptic IIR transfer function,
- order the poles according to the increasing modules,
- $H_\alpha(z)$ encloses the real pole and then every second conjugate complex pair, and
- $H_\beta(z)$ encloses the remaining poles.

We can arbitrarily use: $H_a(z) = H_\alpha(z)$ and $H_b(z)$=$H_\beta(z)$, or $H_a(z) = H_\beta(z)$ and $H_b(z)$=$H_\alpha(z)$. The minimal order of the FIR filter that approximates $H_b(z^{-1})$, n_{FIR}, is obtained when the impulse response of $H_b(z)$ has the minimal value for $n \geq n_{FIR}$. The pole magnitude of the second-order allpass transfer function, ρ, that produces the maximal impulse response at the $n-$th sample versus n, is larger than 0.9 for $n > 10$, as shown in Fig. 10. Usually, the elliptic transfer function has a complex pole-pair with the largest ρ. Therefore, we choose for $H_b(z)$ a transfer function $H_\beta(z)$ or $H_\alpha(z)$ that does not contain the pole with the largest ρ.

For example, for a 12-bit wordlength and the halfband specification (the stopband edge frequency $F_a = 0.28$, the minimal stopband attenuation $A_a = 46\ dB$) and the approximate linear phase design, the impulse response of H_b is smaller than the prescribed acceptable error (2^{-12}) for $n_e = 45$, while for H_a we find $n_e = 177$. Therefore, H_b, used as the time-reversed filter, gives a much smaller L-length sequence, $L = 45$ and the processing delay is $4L = 180$.

The order of the FIR implementation of noncausal subfilter is $n_{FIR} = 45$. The order of the FIR implementation of allpass filter is larger than 177. The order of the optimal linear phase FIR filter, calculated using MATLAB program (`remez`), is $n_{FIR} = 53$. For exact linear phase IIR filter, $H_a = H_b$ as in [15], we find $n_e = 75$ ($\rho_{\max} = 0.7956$) and the processing delay is 300 samples. The optimal FIR filter requires 26 multipliers while the approximate IIR realization requires only 4 multipliers. The phase tolerance

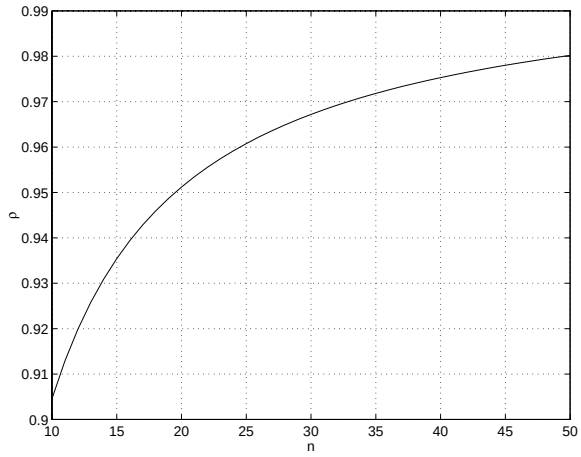

Fig. 10. The pole magnitude of the second-order allpass transfer function, ρ, producing the maximal impulse response at the nth sample.

and the group delay for the approximate linear phase IIR filter are shown in Figs. 11 and 12.

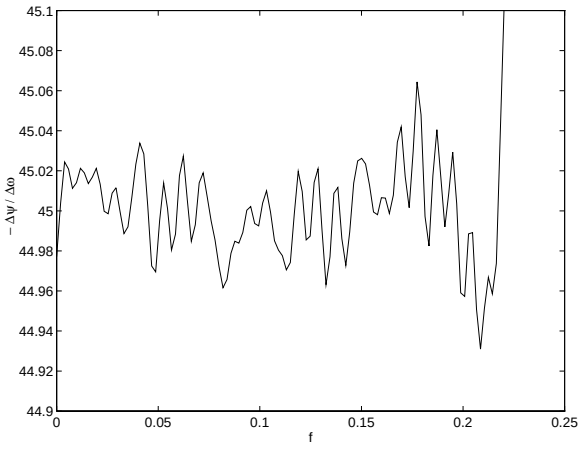

Fig. 11. Group delay (samples) for $L = 45$ and 12-bits wordlength.

8. Design Example and Comparison

In order to compare the complexities and properties of the approximate linear-phase IIR filters satisfying magnitude specification, we take as an example the halfband filter requirements: the stopband edge frequency

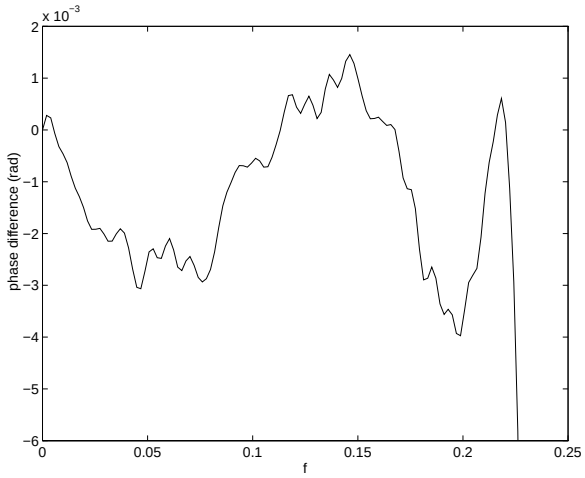

Fig 12. Phase tolerance for $L = 45$ and 12-bits wordlength.

$F_a = 0.28$, the passband edge frequency $F_p = 0.22$, the minimal stopband attenuation $A_a = 46\ dB$, the maximal passband attenuation $A_p = 0.05\ dB$, the approximate linear phase in the passband, the 12-bits data wordlength, and the 10-bits filter coefficient wordlength. We determine the transfer functions $H_\alpha(z)$ and $H_\beta(z)$ using EMQF filter design procedure [17] and obtain

$$H_\alpha(z) = z^{-1}\frac{\beta_1 + z^{-2}}{1+\beta_1 z^{-2}}\frac{\beta_2 + z^{-2}}{1+\beta_2 z^{-2}}, \quad H_\beta(z) = \frac{\beta_3 + z^{-2}}{1+\beta_3 z^{-2}}\frac{\beta_4 + z^{-2}}{1+\beta_4 z^{-2}},$$

$$\beta_1 = \frac{1}{2^2} + \frac{1}{2^3} + \frac{1}{2^6} = 0.390625 \qquad \beta_3 = \frac{1}{2^3} - \frac{1}{2^8} = 0.12109375$$

$$\beta_2 = 1 - \frac{1}{2^3} + \frac{1}{2^6} = 0.890625 \qquad \beta_4 = \frac{1}{2} + \frac{1}{2^3} + \frac{1}{2^5} + \frac{1}{2^7} = 0.6640625$$

Because $\beta_2 > \beta_4$, we use $H_a(z) = H_\alpha(z)$ and $H_b(z) = H_\beta(z)$.

8.1. FIR Implementation of Noncausal Subfilter

We find the 12-bits data wordlength impulse response of $H_b(z)$. According to section 7, we select the first 45 nonzero samples of the impulse response and we create the reversed sequence; this new sequence, $h[n]$, can be used to find the FIR filter that approximate the noncausal IIR filter $z^{-45}H_b(1/z)$: $h[n] = [0.000244140625,\ 0,\ -0.000244140625,\ 0,\ 0.00048828125,\ 0,\ -0.00048828125,\ 0,\ 0.0009765625,\ 0,\ -0.00146484375,\ 0,\ 0.001953125,\ 0,\ -0.0029296875,\ 0,\ 0.004638671875,\ 0,\ -0.0068359375,\ 0,\ 0.01025390625,\ 0,\ -0.015625,\ 0,\ 0.0234375,\ 0,\ -0.035400390625,\ 0,$

0.053466796875, 0, −0.08056640625, 0, 0.12158203125, 0, −0.183349609375, 0, 0.274169921875, 0, −0.3935546875, 0, 0.428955078125, 0, 0.720703125, 0, 0.079833984375].

We quantize the coefficients of $h[n]$ to 10-bits and we use the last 27 nonzero quantized samples. We have used this new sequence, $h_q[n]$, to find the FIR filter that approximate the noncausal IIR filter $z^{-27}H_\beta(1/z)$: $h_q[n] = [-0.0068359375,\ 0,\ 0.0107421875,\ 0,\ -0.015625,\ 0,\ 0.0234375,\ 0,\ -0.03515625,\ 0,\ 0.0537109375,\ 0,\ -0.0810546875,\ 0,\ 0.1220703125,\ 0,\ -0.18359375,\ 0,\ 0.2744140625,\ 0,\ -0.3935546875,\ 0,\ 0.4287109375,\ 0,\ 0.720703125,\ 0,\ 0.080078125]$:

$$\begin{aligned} H_{FIR}(z) = &- 0.0068359375 + 0.0107421875z^{-2} - 0.015625z^{-4} \\ &+ 0.0234375z^{-6} - 0.03515625z^{-8} + 0.0537109375z^{-10} \\ &- 0.0810546875z^{-12} + 0.1220703125z^{-14} - 0.18359375z^{-16} \\ &+ 0.2744140625z^{-18} - 0.3935546875z^{-20} + 0.4287109375z^{-22} \\ &+ 0.720703125z^{-24} + 0.080078125z^{-26} \end{aligned}$$

For the implementation of $H_a(z)$, we use the first-order allpass sections Ansari-Liu from [19]. There are three types of Ansari Liu first-order sections, type a, b and c [19], which behave differently according to overflow. We use the appropriate scaled input and output sequences to prevent the overflow effects: 1/2 for implementing $\left(\beta_1 + z^{-2}\right) / \left(1 + \beta_1 z^{-2}\right)$ by the first-order section Ansari-Liu type a and c; while the scaling factors is $1/2^5$ for type a and $1/2^4$ for type c in the section $\left(\beta_2 + z^{-2}\right) / \left(1 + \beta_2 z^{-2}\right)$. The scaling factors for sections type b are 1.

The filter performances have been tested on the basis of two methods: (1) unit impulse input and FFT of the filter response, and (2) swept sinusoidal input and measured sinusoidal output. The characteristics obtained for the impulse input have larger variations in amplitude than the characteristics obtained for the swept sinusoidal signal as shown in Figs. 13, 14 and 15. The results are obtained by simulation using 10-bits for coefficients and 12-bits for signals. From Figs. 13, 14 and 15, it is evident the choice of the section type is very important, and the best results are obtained with the sections Ansari-Liu type b.

The phase linearity is demonstrated in Fig. 16, where the group delay of $(z^{-26} + H_{FIR}(z)H_a(z))$ for the passband is displayed. Evidently, the group delay variations in the passband are very small and can be neglected in practice (group delay variation $<<$ 1 sample).

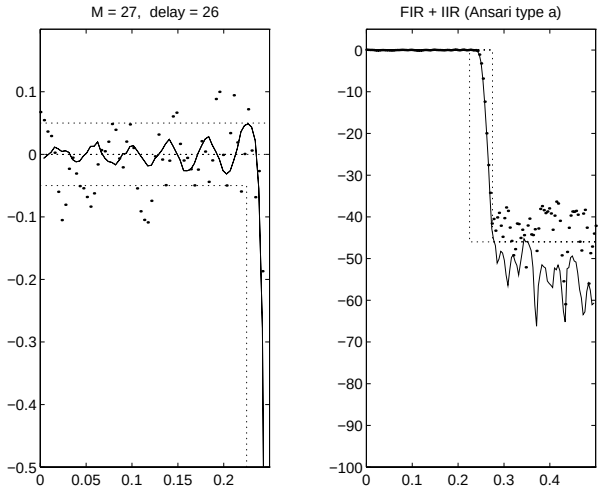

Fig. 13 Spectrum of the filtered signal obtained for impulse input (dotted line) and the amplitude frequency characteristic obtained for the sinusoidal input (solid line): $(z^{-26} + H_{FIR}(z)H_a(z))$, coefficients quantized to 10 bits, signal length 256 samples and 12-bits wordlength, $H_a(z)$ implementedwith Ansari-Liu filter type a.

A new linear phase design has to be compared with optimal linear phase FIR filter. The optimal linear phase FIR filter of the order 53 has been designed, and the results are displayed in Fig. 17. The optimal FIR and $(z^{-26} + H_{FIR}(z)H_a(z))$ have the same average group delay = 26, and approximately the same variation of the attenuation in the passband.

8.2. Time Reversed and Block Processing Technique

We have used the first-order sections Ansari-Liu type b in the time reversed and block processing techniques. Spectrum of the filtered signal obtained for the impulse input has a larger variation than the filter amplitude characteristic measured by the sinusoidal input as shown in Figs. 18 and 19. The simulations have been performed for Ansari-Liu sections type b with 10-bits for coefficients and 12-bits for signals. The passband attenuation is almost ideal with much smaller ripple than in implementations with FIR filters. The number of multiplications per output sample is also several times smaller. With the L-length sequence of block processing technique reduced from $L = 45$ to $L = 27$ the passband attenuation is insignificantly increased but the processing delay is approximately two times smaller.

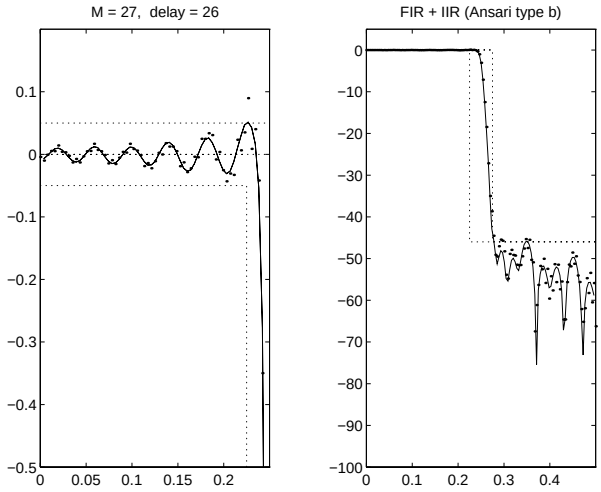

Fig. 14. Spectrum of the filtered signal obtained for impulse input (dotted line) and the amplitude frequency characteristic obtained for the sinusoidal input (solid line): $(z^{-26} + H_{FIR}(z)H_a(z))$, coefficients quantized to 10 bits, signal length 256 samples and 12-bits wordlength, $H_a(z)$ implemented with Ansari-Liu filter type b.

9. Conclusion

In this paper we review the exact and approximate linear phase IIR filter designs and the usage of time-reversed and block processing techniques. We introduce the new design approach based on the classical approximating functions (elliptic, Butterworth and Chebyshev type functions). Using allpass IIR subfilters obtained from the minimal phase solution, we develop a causal filter which approximates simultaneously a constant amplitude response and an exact or approximate linear phase response. The procedure for the calculation of coefficients is based on the procedure for designing classical IIR filters. We have shown that, by a proper selection of the poles of the filter implementing the noncausal IIR filter, the error of the finite representation of the infinite impulse response has a minimal value. The noncausal IIR subfilter is implemented employing an IIR causal subfilter and LIFO registers or FIR subfilters. The application of the proposed design method is demonstrated on the halfband filter example and the effects of the finite wordlength effects have been taken into account.

Design method presented in this paper provides a simple way to reach simultaneously the selective amplitude characteristic and approximately linear phase. The computation procedure does not require any optimization

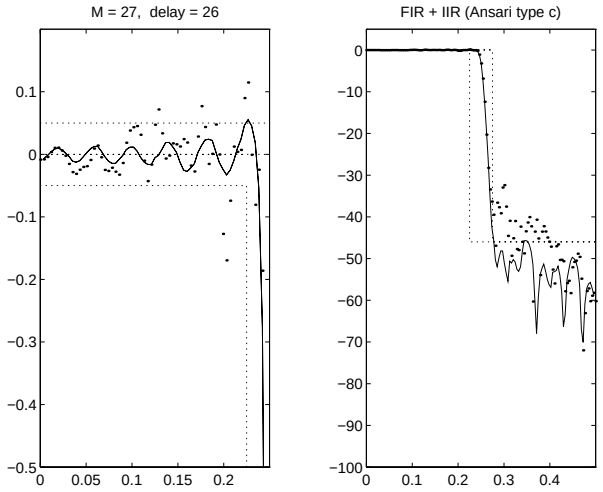

Fig. 15. *Spectrum of the filtered signal obtained for impulse input (dotted line) and the amplitude frequency characteristic obtained for the sinusoidal input (solid line): $(z^{-26} + H_{FIR}(z)H_a(z))$, coefficients quantized to 10 bits, signal length 256 samples and 12-bits wordlength, $H_a(z)$ implemented with Ansari-Liu filter type c.*

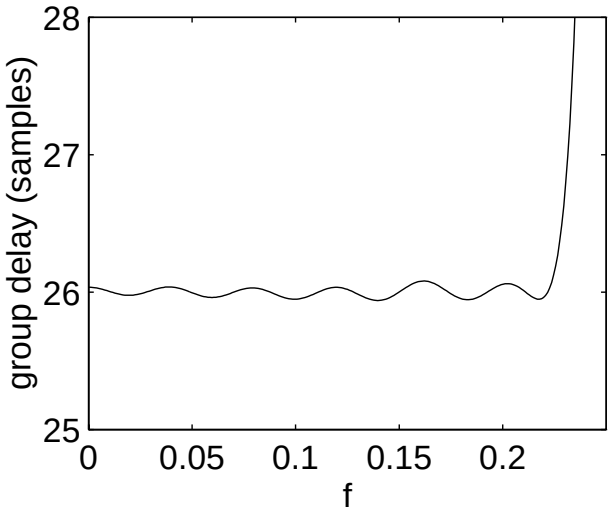

Fig. 16. Group delay of $(z^{-26} + H_{FIR}(z)H_a(z))$: FIR implementation of noncausal subfilter and IIR implementation of causal subfilter.

and therefore is very fast.

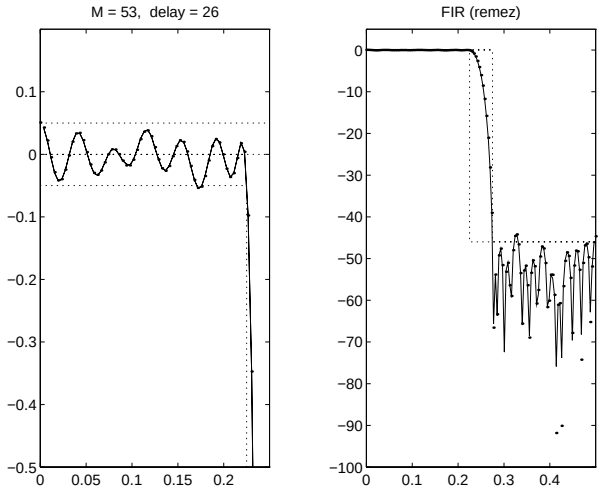

Fig. 17. Spectrum of the filtered signal obtained for impulse input (dotted line) and the amplitude frequency characteristic obtained for the sinusoidal input (solid line): optimal linear phase FIR filter, coefficients quantized to 10 bits, signal length 256 samples and 12-bits wordlength.

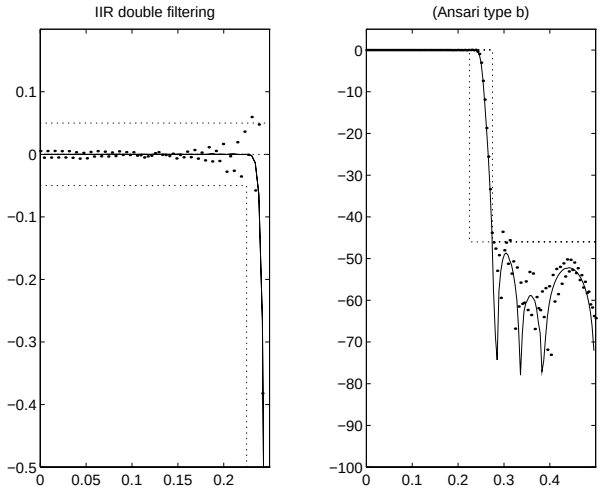

Fig. 18. Spectrum of the filtered signal obtained for impulse input (dotted line) and the amplitude frequency characteristic obtained for the sinusoidal input (solid line): time reversed technique, coefficients quantized to 10 bits, signal length 256 samples and 12-bits wordlength.

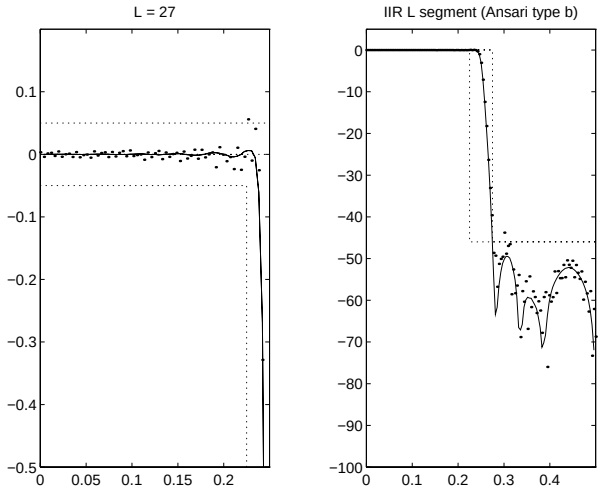

Fig. 19. Spectrum of the filtered signal obtained for impulse input (dotted line) and the amplitude frequency characteristic obtained for the sinusoidal input (solid line): block processing technique, coefficients quantized to 10 bits, signal length 256 samples and 12-bits wordlength.

REFERENCES

1. Z. Jing: *A new method for digital all-pass filter design.* IEEE Trans. Acoust., Speech, Signal Process. vol. ASSP-35, no. 11, pp., 1557–1564, Nov. 1987.

2. L.R. Rabiner and B. Gold: *Theory and application of digital signal processing.* Prentice-Hall, Englewood Cliffs, NJ, 1975.

3. G. Cortelazzo and M.R. Lightner: *Simultaneous design in both magnitude and group delay of IIR and FIR filters based on multiple criterion optimization.* IEEE Trans. Acoust., Speech, Signal Process., vol. ASSP-32, no. 5, pp. 949–967, Dec. 1984.

4. H. Baher: *Digital filters with finite-band approximation to constant amplitude and delay, and arbitrary selectivity.* Proc. IEEE Int. Symp. Circuits Syst. (ISCAS), 1986, pp. 657–659.

5. C.W. Kim and R. Ansari: *Approximately linear phase IIR filters using allpass sections.* Proc. IEEE Int. Symp. Circuits Syst. (ISCAS), 1986, pp. 661–664.

6. M. Renfords and T. Saramaki: *A class of approximately linear phase digital filters composed of all-pass subfilters.* Proc. IEEE Int. Symp. Circuits Syst. (ISCAS), 1986, pp. 678–681.

7. M. Gerken, H.W. Schussler, and P. Steffen: *On the design of recursive digital filters consisting of a parallel connection of allpass sections and delay elements.* AEÜ, Vol.49, No. 1, pp. 1–11, 1995.

8. S.Lawson: *Direct approach to design of PCAS filters with combined gain and phase specifications.* IEE Proc.-Vis. Image Signal Process., Vol.141, No.3, pp. 161–167, June 1994.

9. A. J. Gibbs: *On the frequency domain responses of causal digital filters.*, University of Wisconsin, Madison,WI, PhD thesis, 1969.

10. J. J. Kormylo and V. K. Jain: *Two-pass recursive digital filter with zero phase shift.* IEEE Trans. Acoust., Speech, Signal Processing, vol. ASSP-30, pp. 384–387, Oct. 1974.

11. R. Czarnach: *Recursive processing by noncausal digital filters.* IEEE Trans. Acoust., Speech, Signal Process., vol. ASSP-30, no. 3, pp. 363–370, June 1982.

12. K.P. Estola: *Efficient linear phase FIR filter structures exploiting recursive sub-filters.* Proc. IEEE Int. Symp. Circuits Syst. (ISCAS), 1988, pp. 305–308.

13. P. Jarvilehto and K.P. Estola: *A new modular VLSI filter architecture using computationally efficient recursive digital filter topology.* Proc. IEEE Int. Symp. Circuits Syst. (ISCAS), 1988, pp. 1301–1304.

14. R. Czarnach, H.W. Schussler, and G. Rohrlein: *Linear phase recursive digital filters for special applications.* Proc. IEEE Int. Conf. Acoust. Speech, Signal Processing, 1982, pp. 1825–1828.

15. S. Powell and M. Chau: *A technique for realizing linear phase IIR filters.* IEEE Trans. Signal Process., vol. 39, no. 11, pp. 2425–2435, Nov. 1991.

16. A. N. Willson and H. J. Orchard: *An improvement to the Powell and Chau linear phase IIR filters.* IEEE Trans. Signal Processing, vol. SP-42, no. 10, pp. 2842–2848, Oct. 1994.

17. Lj. Milić and M. Lutovac: *Design of multiplierless elliptic IIR filters with a small quantization error.* IEEE Trans. Signal Processing, vol. 47, no. 2, pp. 469–479, Feb. 1999.

18. B. Djokić, M. Popović, and M. Lutovac: *A new improvement to the Powell and Chau linear phase IIR filters.* IEEE Trans. Signal Processing, vol. 46, no. 6, pp. 1685–1688, June 1998.

19. R. Ansari and B. Liu: *A class of low-noise computationally efficient recursive digital filters with applications to sampling rate alterations.* IEEE Trans. Acoust., Speech, Signal Process., vol. ASSP-33, no. 1, pp. 90–97, Feb. 1985.